



12

DA 114068

# MONOLITHIC GaAs DUAL-GATE FET PHASE SHIFTER

RCA Laboratories  
Princeton, New Jersey 08540

FEBRUARY 1982

TRI-ANNUAL REPORT NO. 4  
for the period 1 September 1981 to 31 December 1981

Approved for public release; distribution unlimited.  
Reproduction, in whole or in part, is permitted  
for any purpose of the U.S. Government.

Prepared for  
Department of the Navy  
Office of Naval Research  
Arlington, Virginia 22217  
Contract No. N00014-79-C-0568

DTIC  
ELECTE  
S MAY 18 1982 D  
E

DTIC FILE COPY

82 05 18 084



PREFACE

This Tri-annual Report describes the work performed under Contract No. N00014-79-C-0568 during the period 1 September 1981 to 31 December 1981 in the Microwave Technology Center, F. Sterzer, Director. H. C. Huang is the project supervisor, and M. Kumar is the project scientist.

Accession For	
NTIS GRA&I	<input checked="" type="checkbox"/>
DTIC TAB	<input type="checkbox"/>
Unannounced	<input type="checkbox"/>
Justification	
By _____	
Distribution/	
Availability Codes	
Dist	Avail and/or Special
A	



## TABLE OF CONTENTS

Section	Page
I. OBJECTIVE .....	1
II. PROGRESS .....	1
A. 90° Monolithic Dual-Gate FET Phase Shifter .....	1
B. 360° Phase Shifter .....	1
C. Processing Details of the Dual-Gate FET Phase Shifter .....	5
III. PUBLICATIONS .....	8
Appendices	
A. Broad-Band Active Phase Shifter Using Dual-Gate MESFET .....	9
B. Planar Broad-Band 180° Hybrid Power Divider/Combiner Circuit .....	14

## LIST OF ILLUSTRATIONS

Figure	Page
1. Photograph of the 90° monolithic dual-gate FET phase shifter ....	2
2. 360° phase shifter (old design) .....	3
3. 360° phase shifter .....	3
4. 360° phase shifter (new design) .....	4
5. Cross-sectional view of the capacitor .....	5
6. Circuits defined .....	5
7. Circuits plated .....	6
8. Posts defined .....	6
9. Posts plated .....	6
10. Air bridge defined .....	7
11. Air bridge plated .....	7
12. Completed air bridge .....	8

## I. OBJECTIVE

The objective of this four-year program (Sept. 1, 1979 to Aug. 31, 1983) is to develop a monolithic GaAs dual-gate FET phase shifter, operating over the 4- to 8-GHz frequency band and capable of a continuously programmable phase shift from  $0^\circ$  through  $N$  times  $360^\circ$  where  $N$  is an integer. The phase shift is to be controllable to within  $\pm 3^\circ$ . This phase shifter will be capable of delivering an output power up to 0 dBm with an input and output VSWR of less than 1.5:1.

## II. PROGRESS

In Tri-Annual Report No. 3 for the period 1 May 1981 to 31 August 1981, we reported the progress in the development of a  $90^\circ$  interdigitated coupler. Two couplers were reported: a  $25\text{-}\Omega$ , 6-line coupler and a  $50\text{-}\Omega$ , 4-line coupler. The performance of these couplers was quite satisfactory.

### A. $90^\circ$ Monolithic Dual-Gate FET Phase Shifter

During this reporting period, we have completed the fabrication of a 0 to  $90^\circ$  monolithic phase shifter. The photograph of the phase shifter chip is shown in Fig. 1. We are in the process of evaluating the rf characteristics of the various components and the overall phase shifter.

### B. $360^\circ$ Phase Shifter

In Tri-Annual Report No. 1 (for the period 1 September 1980 to 31 December 1980) we reported the design, fabrication, and performance of the  $360^\circ$  phase shifter using discrete components in MIC format. We have conceived a modified design of the  $360^\circ$  phase shifter which uses fewer hybrids and thus reduces the overall size of the monolithic  $360^\circ$  phase shifter. The earlier approach, illustrated in Fig. 2, used a  $180^\circ$  hybrid (Appendix B), two  $90^\circ$  hybrids, and a four-to-one-way, in-phase combiner. There is another approach, as illustrated in Fig. 3, for obtaining four orthogonal vectors. In this approach a  $90^\circ$  hybrid is replaced by a  $180^\circ$  hybrid and vice versa. Each  $180^\circ$  hybrid in Fig. 3 can be replaced by two  $90^\circ$  hybrids, one at the input end and the other at the output end of the dual-gate FET amplifier. This is shown in Fig. 4.

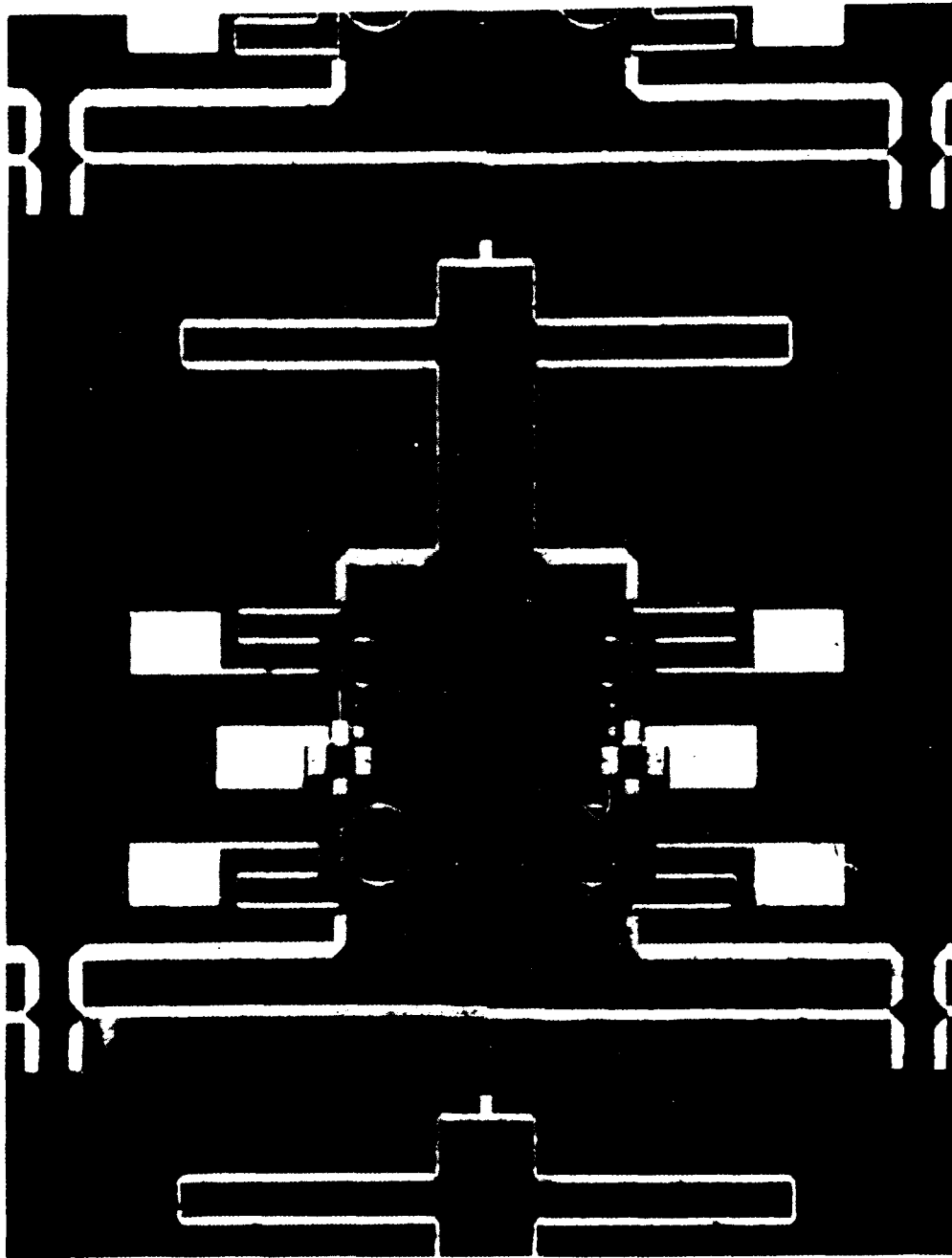


Figure 1. Photograph of the 90° monolithic dual-gate FET phase shifter.

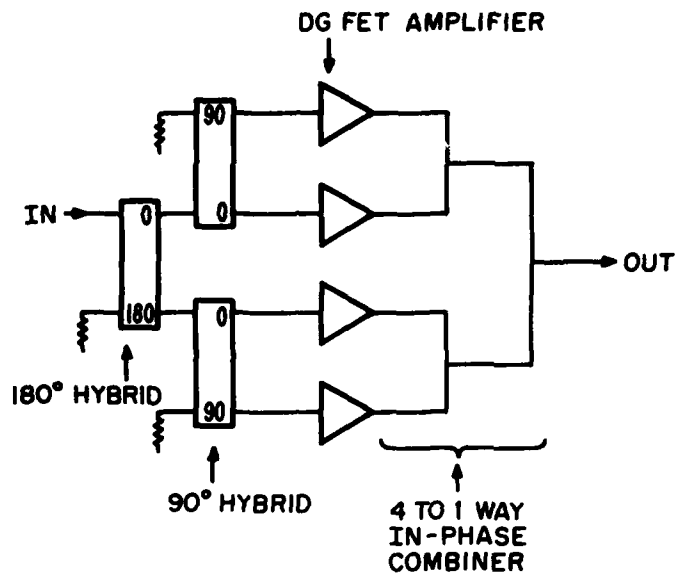


Figure 2. 360° phase shifter (old design).

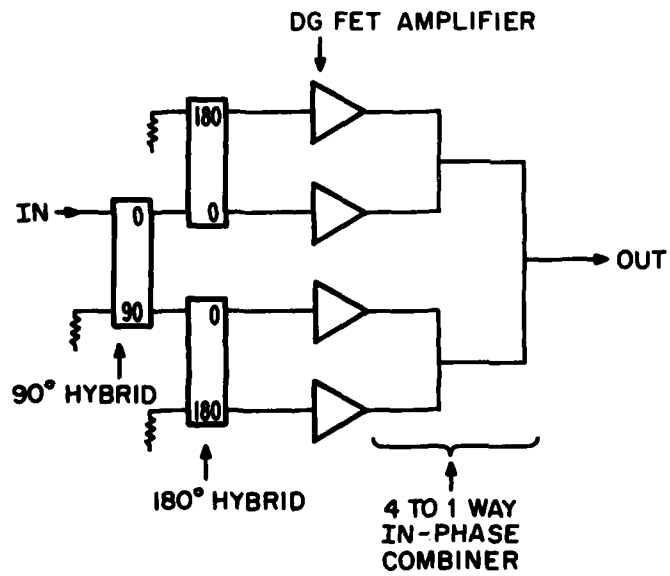


Figure 3. 360° phase shifter.

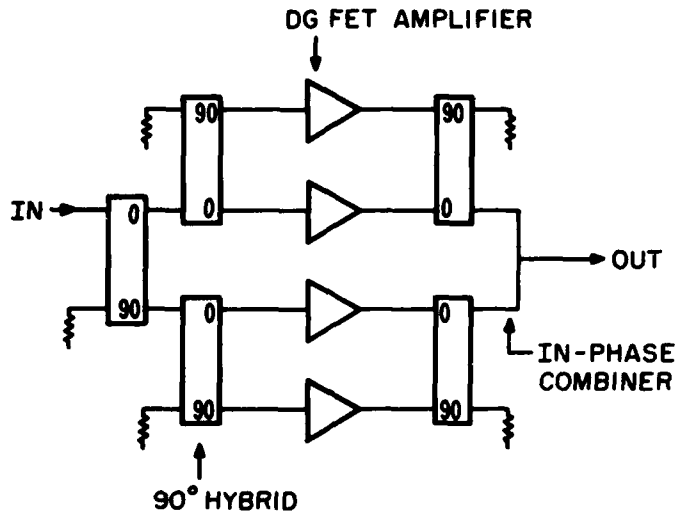


Figure 4. 360° phase shifter (new design).

This new configuration of the 360° phase shifter uses only one two-to-one-way, in-phase combiner as compared to the four-to-one-way combiner, which consists of three two-to-one-way combiners, used in the earlier design (Fig. 2). The total number of 90° hybrids in the new design (Fig. 4) is the same as that used in the earlier design (Fig. 2), since the 180° hybrid consists of three 90° hybrids (Appendix B). Therefore, the new design reduces the overall size of the phase shifter significantly. Folded 90° hybrids (interdigitated hybrids) will be used in the design of the 360° phase shifter.

The two 90° interdigitated hybrids used at the output of the dual-gate FET amplifier can have the input/output impedances lower than 50 Ω (e.g., 25 Ω) since an in-phase combiner can easily be designed with different input and output impedances. Use of a 25-Ω, 90° hybrid will reduce the loss and size of the matching network of the output impedance of the dual-gate FET. We reported the development of the 25-Ω, 90° interdigitated hybrid in Tri-Annual Report No. 3. The overall estimated dimensions of the 360° phase shifter are 7 mm x 7 mm x 0.1 mm. The design of this phase shifter is in progress.

### C. Processing Details of the Dual-Gate FET Phase Shifter

The phase shifter is initially fabricated on a 10- to 12-mil-thick GaAs wafer. We have used both ion-implanted and epitaxially grown wafers for processing the dual-gate FETs. The ohmic contact metallization is Au-Ge/Ni/Au sintered at 450°C for 1 minute. The metallization for the gates as well as the bottom plates of the capacitors is Ti/Pt/Au. After the FETs are fabricated, a thin layer of  $\text{Si}_3\text{N}_4$  (2800 Å) is sputter-deposited. This layer serves not only as the dielectric material for the capacitors but also as a passivation layer for the FETs. Then 2000 Å of Ti and 200 Å of Au are evaporated on the whole surface. This facilitates the plating of the circuits (such as the couplers and top plates of the capacitors). In addition, the 2000-Å Ti is used to define the resistors.

Figure 5 shows a cross-sectional view of the capacitor. The circuits are defined in thick photoresist and gold-plated to a thickness of about 4 to 5  $\mu\text{m}$  (Figs. 6 and 7). Posts are defined in thick photoresist and plated to a thickness of about 3  $\mu\text{m}$  (Figs. 8 and 9). A thin layer of Au (200 to 300 Å) is evaporated onto the surface, air bridges defined in thick photoresist, and plated to a thickness of about 2 to 3  $\mu\text{m}$  (Figs. 10 and 11).

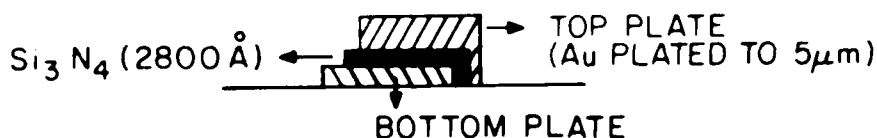


Figure 5. Cross-sectional view of the capacitor.

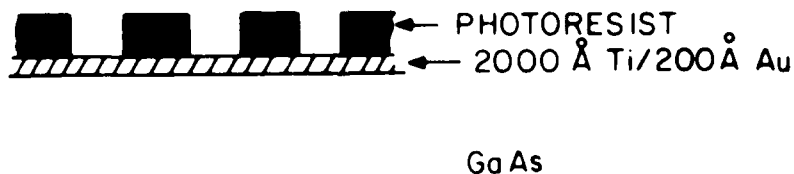


Figure 6. Circuits defined.



GaAs

Figure 7. Circuits plated.



Figure 8. Posts defined.



Figure 9. Posts plated.

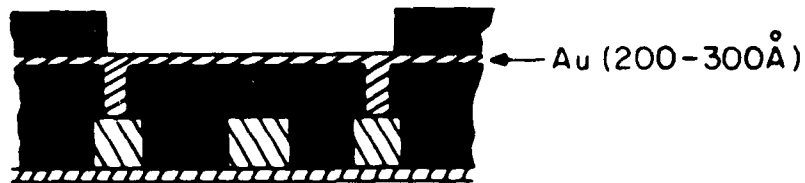


Figure 10. Air bridge defined.

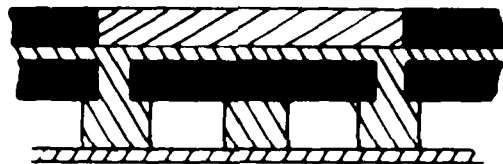


Figure 11. Air bridge plated.

We have observed that during the plating of the posts there is a tendency for the thick photoresist to crack making the alignment with the air-bridge mask difficult if not impossible. Simultaneous with the standard technique for fabricating the air bridges, we have been trying alternate process techniques such as underbridges with insulators.

After the completion of the air bridge, the bottom Au layer is etched off. The resistors are defined and protected, and the rest of the Ti is etched off (Fig. 12).

The wafer is thinned down to 4 mil and via holes are drilled using a laser. The bottom surface of the wafer is metallized and plated up through the via holes. The wafer is diced and ready for measurements.

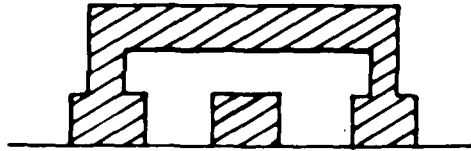


Figure 12. Completed air bridge.

### III. PUBLICATIONS

The following papers have been published since the last reporting period:

1. M. Kumar, R. J. Menna and H. C. Huang, "Broad Band Active Phase Shifter Using Dual-gate MESFET," IEEE Transactions on Microwave Theory and Techniques, Vol. MTT-29, No. 10, pp. 1098-1102, October 1981.
2. M. Kumar, R. J. Menna and H. C. Huang, "Planar Broad Band 180° Hybrid Power Divider/Combiner Circuit," IEEE Transactions on Microwave Theory and Techniques, Vol. MTT-29, No. 11, pp. 1233-1235, November 1981.

Copies of these papers are included as Appendices A and B.

### Broad-Band Active Phase Shifter Using Dual-Gate MESFET

MAHESH KUMAR, MEMBER, IEEE, RAYMOND J. MENNA,  
MEMBER, IEEE, AND HO-CHUNG HUANG, SENIOR MEMBER, IEEE

*Abstract*—This paper describes a broad-band, dual-gate MESFET phase shifter (vector generator), operating over the 4–8-GHz frequency band and capable of a continuous phase shift and multiplicity of modulations including digital phase shift and amplitude modulation directly, and indirectly (with additional information processing circuits), single sideband modulation, frequency modulation, and phase modulation, etc. A dual-gate FET is

Manuscript received April 7, 1981; revised June 3, 1981. This work was supported by the Office of Naval Research under Contract N00014-79-C-0568. The authors are with RCA Laboratories, David Sarnoff Research Center, Princeton, NJ 08540.

used as a variable gain amplifier and phase shift is obtained by complex addition of two orthogonal variable vectors. The principle of the phase shifter and the experimental results are presented.

#### I. INTRODUCTION

In the past, ferrite phase shifters have been used in the phased array radar systems. The p-i-n diode phase shifters are being considered because of their lighter weight, higher speed, and transmission reciprocity as compared to the ferrites [1]–[4]. The ferrite and p-i-n diode phase shifters, however, still suffer from a relatively slow response time. The recent interest in fully active phased array radars as well as progress in the monolithic GaAs integrated circuits has opened the possibility of realizing active phase shifting subassemblies based upon GaAs field-effect transistors (FET's).

The dual-gate FET has been used in many applications such as variable-gain amplifiers [5], power limiters [6], discriminators [7], and mixers [8], etc. A single-frequency dual-gate FET phase shifter has been reported [9], [10]. The phase shift is obtained by changing the dc voltage applied to the control gate of the FET, and a linear phase shift of  $100^\circ$  has been obtained at a single frequency of 12 GHz. A phase shift of up to  $140^\circ$  was obtained using a three-device amplifier phase shifter assembly [11]. Pengelly *et al.* [12], studied the transmission phase variation of a gain-controlled, dual-gate GaAs MESFET's amplifier, at S-band, which depends upon the nature of the matching circuits used in the amplifier. These types of phase shifters are, in principle, capable of a relatively narrow bandwidth.

A narrow-band phase shifter, using a different operating principle, has also been reported [4], [13], [14]. The phase shift in this case is obtained by complex vector addition of two orthogonal vectors. This circuit operates over a bandwidth of 1 GHz in the X-band. There is yet another possibility of using three variable-gain amplifiers to obtain a  $360^\circ$  phase shift by using a vector sum of three nonorthogonal signals separated by  $120^\circ$  each [15]. This approach could lead to a small size, but it is potentially more suitable for narrow-band applications.

This paper presents the design and development of an octave bandwidth, dual-gate FET phase shifter operating over the 4–8-GHz band, capable of a continuous phase shift from zero through  $N$  times  $360^\circ$  where  $N$  is an integer. The phase shift is obtained by the vector sum of four orthogonal signals whose amplitudes can be varied over a wide dynamic range. Four dual-gate FET amplifiers are used as variable-gain amplifiers for the amplitude control. The overall amplitude of the phase shifter can be varied by properly adjusting the gate voltages of the dual-gate FET amplifiers. Thus a signal of any phase and amplitude can be generated. Hence, the phase shifter can be used as a vector generator. This phase shifter has been realized on a microstrip circuit, and is compatible to monolithic integration on a GaAs substrate. The work on developing the monolithic phase shifter is in progress [16], [17].

The phase shifter reported here offers several advantages such as 1) minimal loss: because of the inherent high gain capability of the dual-gate FET, various signal processing such as switching and  $180^\circ$  phase inverting can be accomplished with very little loss; 2) fast response: the response time of a dual-gate FET is of the order of a few hundred picoseconds. This fast response characteristic will lead to high-speed operation; 3) capability of extending to high bits: the key element of the phase shifter is an analog  $90^\circ$  phase shifter employing two dual-gate FET's. It is feasible to increase the number of bits by changing the control voltages to the second gates; 4) serrodyning for Doppler shift can be readily performed using this phase shifter; 5) the phase shifter has application in biphasic modulation for secure communications or coding and beam steering.

## II. PRINCIPLE OF PHASE SHIFTER

### A. $90^\circ$ Phase Shifter

The key element of the  $360^\circ$  phase shifter is an analog  $90^\circ$  phase shifter employing two dual-gate FET's. The conceptual design of the  $90^\circ$  phase shifter is shown in Fig. 1. The two dual-gate FET amplifiers are excited in quadrature phase through a hybrid power splitter at a designated RF frequency. The outputs of both FET amplifiers are then combined through an in-phase power combiner to produce a phase-controlled output. The two dual-gate FET amplifiers are used as variable gain amplifiers [5]. It has been shown earlier that the gain of a

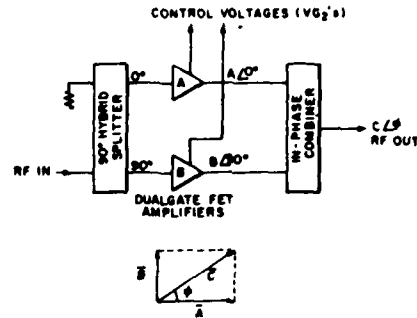


Fig. 1 Schematic of a  $90^\circ$  GaAs dual-gate FET phase shifter

dual-gate FET amplifier can be controlled from  $+10$  to  $-30$  dB (cutoff) by controlling the second gate bias voltage [5]. The phase difference in path A and path B (Fig. 1) is  $90^\circ$ . The resulting vector sum of the two combined quadrature RF signals is given by

$$C = A + B \quad (1)$$

$$C \angle \phi = A + jB = |C| \angle \tan^{-1} B/A \quad (2)$$

where  $C$  is the resultant RF voltage amplitude and  $\phi$  is the phase angle. The output phase angle is, therefore, controlled by adjusting the relative amplitudes of the quadrature vectors  $A$  and  $B$ . This is accomplished by independently adjusting the gain of each of the dual-gate FET amplifiers.

For most system requirements, the absolute amplitude of the resulting phase shifted RF signal must be kept constant, independent of the selected output phase angle. This means that  $|C|$  is invariant and the phase angle is selected by controlling the amplitudes of both RF signals  $A$  and  $B$ . For this unique requirement

$$\sqrt{A^2 + B^2} = \text{constant} \quad (3)$$

This can be obtained by partially biasing the amplifiers  $A$  and  $B$  such that output is at the 0.707 level. The overall amplitude of the phase shifter can be varied by changing the gate voltages of both amplifiers simultaneously. Thus in (3), the constant output amplitude level can be varied and this phase shifter becomes a vector generator. A vector generator is a device where a vector of any phase or amplitude (with respect to an input reference signal) could be generated.

### B. $360^\circ$ Phase Shifter

Fig. 2 illustrates the schematic of a continuously variable  $0^\circ$  to  $360^\circ$  phase shifter. The  $360^\circ$  phase shift is achieved by the sum of four quadrature vectors  $A \angle 0^\circ$ ,  $B \angle 90^\circ$ ,  $C \angle 180^\circ$ , and  $D \angle 270^\circ$  with properly controlled amplitudes of  $A$ ,  $B$ ,  $C$ , and  $D$ . Those four quadrature vectors can be realized by a  $180^\circ$  power divider, two  $90^\circ$  hybrids, four dual-gate FET amplifiers and an in-phase, four-way power combiner as shown in Fig. 2. The incoming signal is first divided into two signals which are equal in amplitude but  $180^\circ$  apart in phase. Then each signal is further divided into two signals through a  $90^\circ$  hybrid, resulting in four signals of equal amplitude and having phases of  $0^\circ$ ,  $90^\circ$ ,  $180^\circ$ , and  $270^\circ$ . Each signal is then amplified through a dual-gate FET amplifier, and the four outputs are then combined through a four-way, in-phase combiner to obtain a phase-controlled output. Fig. 2 illustrates the four quadrants of  $360^\circ$  phase shift which are

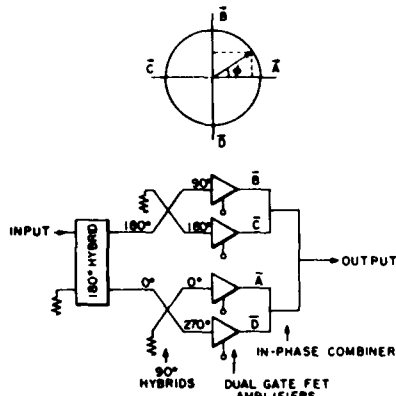


Fig. 2. Schematic of a 360° GaAs dual-gate FET phase shifter.

obtained using a combination of two vectors at a time. Each dual-gate FET serves as an amplifier-switch which can control the amplitudes of the vectors  $A$ ,  $B$ ,  $C$ , and  $D$ . As an example, when  $C$  and  $D$  are switched off,  $A$  and  $B$  are switched on, an output signal with about 30° phase advance relative to the input signal is obtained (Fig. 2). By changing the second gate bias voltages of amplifiers  $A$  and  $B$  (when  $C$  and  $D$  are switched off), the total 0° to 90° phase shift can be obtained. Thus by controlling the bias voltages of two amplifiers at one time, while the other two are switched off, the total of 360° continuous phase shift is obtained.

It is appreciated that

$$\omega = \frac{d\phi}{dt} \quad (4)$$

Thus by applying varying potentials to the control gates, the phase can be continuously rotated at a given rate resulting in an output frequency which is offset in frequency from the input frequency. It can be shown that by proper choice of input signals to the four control gates, the following modulation functions may be performed: a) amplitude modulation; b) pulse code modulation; c) frequency modulation; d) phase modulation; e) continuous phase modulation; f) biphasic shift keying; g) quadrature phase shift keying; h) multiphase shift keying; i) single-side band modulation; and j) combination of above.

### III. DESIGN, FABRICATION AND PERFORMANCE

The design of the 360° phase shifter involves the design of the following components: 180° hybrid, 90° hybrid, four-way combiner, and dual-gate FET amplifier. A 180° planar hybrid is realized using a 90° interdigitated hybrid and a 0-dB tandem coupler [18]. A 0-dB tandem coupler consists of two, 3-dB 90° interdigitated hybrids connected in tandem (side-by-side) which produces a 0-dB coupling [19]. The schematic of the 180° hybrid is shown in Fig. 3. It is a four-port device. Ports 1 and 2 are the input ports and ports 3 and 4 are the output ports. When the signal is fed to port 1, with port 2 match terminated, the signals appearing at ports 3 and 4 are both 3 dB below the input signal and have a phase difference of 180°. This hybrid has a 3-GHz bandwidth over the 4–8-GHz band, and a phase unbalance of  $\pm 7^\circ$ . The designs of the 90° interdigitated hybrid and a four-way Wilkinson power combiner are standard and are not discussed

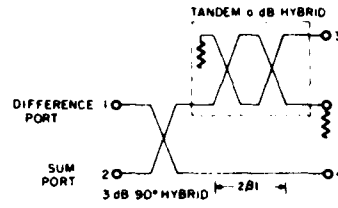


Fig. 3. Schematic of a 180° hybrid.

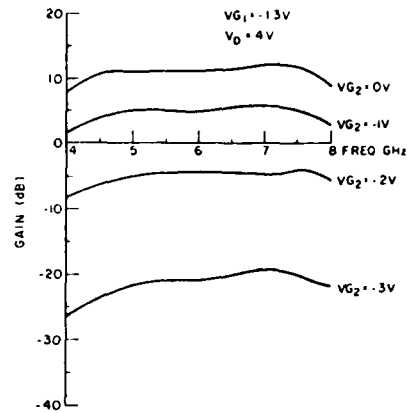
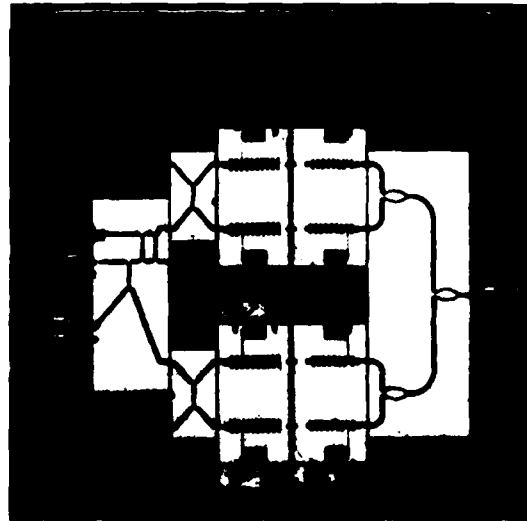
Fig. 4. Variation of gain versus voltage ( $V_{G2}$ ) of a dual-gate FET amplifier.

Fig. 5. Photograph of the 360° phase shifter.

here. The dual-gate FET amplifier design is done using CAD techniques [5]. Fig. 4 shows the variation of gain with frequency for different second gate bias voltages. The gain of the amplifier can be varied from 10 to -30 dB (cutoff) by changing the second gate (control gate) bias voltage. The photograph of the 360°

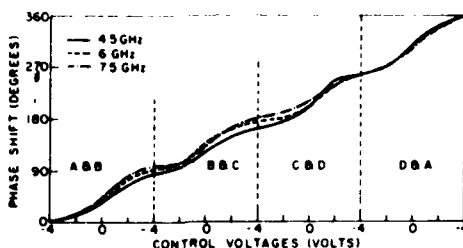


Fig. 6. Variation of phase with control voltages of 360° phase shifter

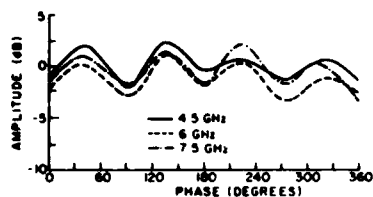


Fig. 7. Variation of amplitude with phase of 360° phase shifter.

phase shifter is shown in Fig. 5. All the passive circuit components such as the 90° and 180° hybrids, Wilkinson four-way power combiner and dc bias circuits of the dual-gate FET's are designed in the planar form so that the complete phase shifter can readily be integrated on a monolithic GaAs chip. Fig. 6 shows the variation of phase shift with control voltages (the second gate bias voltages). The 0° to 360° continuous phase shift is obtained by changing the second gate bias voltages of the dual-gate FET amplifiers in a systematic manner. Referring to Fig. 6, there are four sections which divide the total phase shift of 360° by four dotted, vertical lines. Each section represents the phase control of one quadrant. In each quadrant, the control voltages of two dual-gate FET amplifiers are varied, while the remaining two amplifiers are switched off by applying -4 V [5] to their second gates. For example, in the first quadrant, the  $V_{G2}$ 's for A and B are varied while the  $V_{G2}$ 's for C and D are kept at -4 V for switched-off conditions. Now to get a 90° phase shift, amplifier A is kept under the on condition ( $V_{G2}(A)=0$  V) and  $V_{G2}(B)$  for amplifier B is varied from -4 to 0 V which gives approximately the 45° phase shift (Fig. 6). Next, amplifier B is switched on ( $V_{G2}(B)=0$  V) and the  $V_{G2}(A)$  for amplifier A is varied from 0 to -4 V which gives approximately from 45° to 90° phase shift. Thus controlling the two second gate bias voltages of two amplifiers, a 90° phase shift is obtained. This process is repeated with other combinations of two orthogonal vectors to obtain the entire 0° to 360° phase shift.

The variation of amplitude with phase is presented in Fig. 7. The gain of the phase shifter is plotted as a function of phase for different frequencies. The maximum variation of gain is  $\pm 3$  dB for a 360° phase shift. As explained earlier, the phase shift at 0°, 90°, 180°, and 270° is obtained by switching three amplifiers off while leaving only one amplifier on; this gives a variation of 5 dB in amplitude because of the four-way power combination characteristic [20], [21]. It is possible to achieve a constant output power for any given phase by partially biasing two amplifiers instead of biasing only one amplifier at a time and keeping others off. This was explained in Section II (3).

#### IV. CONCLUSIONS

A broad-band active phase shifter has been presented, operating over the 4–8-GHz band. The 360° continuous phase shift is obtained with minimal loss. The phase shifter design presented here is compatible to monolithic integration on GaAs substrates. This phase shifter has several advantages over other kinds of phase shifters—in light weight, fast response, low loss, and octave bandwidth capability. It can be used as a vector generator if the amplitude of the signal is varied along with phase.

#### ACKNOWLEDGMENT

The authors wish to thank E. Mykietyń and P. A. Czajkowski for their help in the assembly of the phase shifter.

#### REFERENCES

- [1] Mark E. Davis, "Integrated diode phase-shifter elements for an X-band phased-array antenna," *IEEE Trans. Microwave Theory Tech.*, vol. MTT-23, pp. 1080–1084, Dec. 1975.
- [2] A. Rosen *et al.*, "High power, low-loss PIN diodes for phased-array radar," *RCA Rev.*, vol. 40, no. 1, pp. 22–58, Mar. 1979.
- [3] R. V. Garver, *Microwave Diode Control Devices* Artech House, 1976, pp. 287–291.
- [4] ———, "PIN diode single-sideband modulation," in *IEEE-GMTT Int. Microwave Symp. Dig.*, pp. 235–238, May 1970.
- [5] M. Kumar and H. C. Huang, "Dual-gate MESFET variable-gain, constant-output power amplifier," *IEEE Trans. Microwave Theory Tech.*, vol. MTT-29, pp. 185–189, Mar. 1981.
- [6] A. Rosen, H. Wolkstein, J. Goel, and R. J. Matarese, "A dual-gate GaAs FET RF power limiter," *RCA Rev.*, vol. 38, June 1977.
- [7] R. S. Pengelly, "Broadband and narrow-band frequency discriminators using dual-gate GaAs FETs," in *9th European Microwave Conf. Proc.*, (Brighton, England), pp. 326–330, Sept. 1979.
- [8] C. Tsironis *et al.*, "A self-oscillating, dual-gate MESFET X-band mixer with 12 dB conversion," in *9th European Microwave Conf. Proc.*, (Brighton, England), pp. 321–325, Sept. 1979.
- [9] C. Tsironis and P. Harrop, "Dual-gate MESFET phase shifter with gain at 12 GHz," *Electron. Lett.*, vol. 16, no. 14, pp. 553–554, July 3, 1980.
- [10] C. Tsironis and P. Harrop, "Phase shifters with dual-gate MESFETs," in *Proc. European Solid State Circuits Conf.*, pp. 212–214, (Grenoble), 1980.
- [11] C. Tsironis *et al.*, "Active phase shifters at X-band using GaAs MESFETs," in *IEEE Int. Solid-State Circuits Conf. Dig.*, pp. 140–141, (New York), 1981.
- [12] R. S. Pengelly *et al.*, "Performance of dual-gate GaAs MESFETs as phase shifters," in *IEEE Int. Solid-State Circuits Conf. Dig.*, pp. 142–143, (New York) 1981.
- [13] M. J. Fithian, "Two microwave complex weighting circuits," in *IEEE MTT-S Int. Microwave Symp. Dig.*, pp. 126–128 (Washington, DC), May 28–30, 1980.
- [14] "S-band complex-weight module for adaptive processing," NASA Tech. Brief-LAR-12197, spring 1978.
- [15] Y. Gazit and H. C. Johnson, "A continuously-variable Ku-band phase/amplitude module," presented at the 1981 IEEE MTT-S Int. Microwave Symp., (Los Angeles, CA), June 15–17, 1981.
- [16] M. Kumar, G. Taylor and H. Huang, "Design considerations for monolithic GaAs FET amplifier," presented at the GaAs IC Symp., (Las Vegas, Nevada), Nov. 4–6, 1980.
- [17] "Monolithic dual-gate GaAs FET amplifier," *IEEE Trans. Electron Devices*, vol. ED-28, pp. 197–198, Feb. 1981.
- [18] M. Kumar, R. J. Menna and H. C. Huang, "Planar hybrid power divider/combiner circuit," to be published.

- [19] W. S. Moselett, "Cascading 4-port networks," *Microwave J.*, vol. 12, pp. 77-82, Sept. 1969.
- [20] R. L. Ernst, R. L. Combs, and A. Presser, "Graceful degradation properties of matched  $n$ -port power amplifier combiners," in *MTT-S Int. Microwave Symp. Dig.*, pp. 174-177, June 1977.
- [21] A. A. M. Saleh, "Improving the graceful-degradation performance of combined power amplifiers," *IEEE Trans. Microwave Theory Tech.*, vol. MTT-28, pp. 1068-1070, 1980.

## APPENDIX B

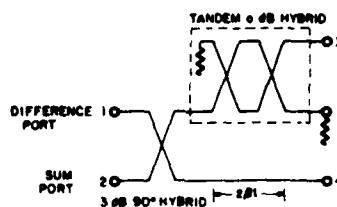


Fig. 1 Schematic of a 180° hybrid

### I. INTRODUCTION

In the past, 180° hybrids have been extensively used in balanced mixers, switching networks, phase shifters, and push-pull amplifiers. The recent interest in monolithic GaAs integrated circuits has opened the need for a 180° planar hybrid compatible to monolithic integration on GaAs substrates.

Conventional hybrid rings have been used as 180° hybrids. The hybrid ring has a narrow bandwidth. Reflection-type 180° hybrids have been reported in literature [1]. The problem with this kind of hybrid is the practical difficulty of realizing a good short or open circuit over wide band of frequencies. The commercially available 180° hybrids use a tandem connection of two couplers using broadside coupling [2], [3]. This is a multilayer structure and can be realized using striplines only. Recently, a 3-dB 180° hybrid has been reported [4] which uses a slot line-microstrip coupling. The abovementioned structures for 180° hybrids are not planar, and not easily compatible to monolithic circuit fabrication.

This paper presents an analysis and experimental results of a broad-band 180° planar hybrid. This hybrid is a four-port device with two input ports and two output ports. One of the input ports is designated as the sum port and the other as the difference port. A signal fed into the sum port or the difference port is divided into two signals of equal amplitude with a phase difference of 0° or 180°, respectively. This hybrid has been realized using a 3-dB interdigitated, 3-dB 90° hybrid, and a 0-dB 90° interdigitated tandem hybrid. The latter hybrid introduces an additional 90° phase shift which is independent of frequency. The analysis of the circuit is presented in Section II. The hybrid has been designed and fabricated on alumina substrate for C-band operation. The experimental results are presented in Section III.

### II. ANALYSIS OF THE HYBRID

The schematic of the hybrid is shown in Fig. 1. It is a four-port device. Ports 1 and 2 are the input ports and ports 3 and 4 are the output ports. When the signal is fed to port 1, the signals appearing at port 3 and port 4 are both 3 dB below the input signal and have a phase difference of 180°. When a signal is fed at port 2, the signals appearing at ports 3 and 4 are both 3 dB below the input signal and are in phase. These two cases are considered separately and the analysis is presented for both cases.

#### Case 1: Input at Difference Port

Let  $\theta$  be the coupling angle and  $l$  be the coupling length. The hybrid is illustrated in Fig. 1. Port 4 has an extra length of transmission line of length  $2\beta l$ . It will be shown later that the phase difference of the two output signals appearing at ports 3 and 4 is independent of frequency. Assume that a unit amplitude signal is fed at port 1 (port 2 is theoretically isolated), then the

### Planar Broad-Band 180° Hybrid Power Divider/Combiner Circuit

MAHESH KUMAR, MEMBER, IEEE, RAYMOND J. MENNA, MEMBER, IEEE, AND HO-CHUNG HUANG, SENIOR MEMBER, IEEE

**Abstract**—A planar broad-band 180° hybrid is presented. The hybrid is realized using a 3-dB 90° hybrid and a 0-dB 90° tandem hybrid. An interdigitated version of the hybrid fabricated on alumina substrate performed well over the 4–8-GHz band. The hybrid has an insertion loss of 0.5 dB, phase imbalance of  $\pm 7^\circ$ , and an isolation of better than 18 dB over the band.

Manuscript received April 7, 1981; revised July 13, 1981. This work was supported by the Office of Naval Research, Arlington, VA, under Contract N00014-79-0568, and monitored by M. N. Yoder.

The authors are with RCA Laboratories, David Sarnoff Research Center, Princeton, NJ 08540.

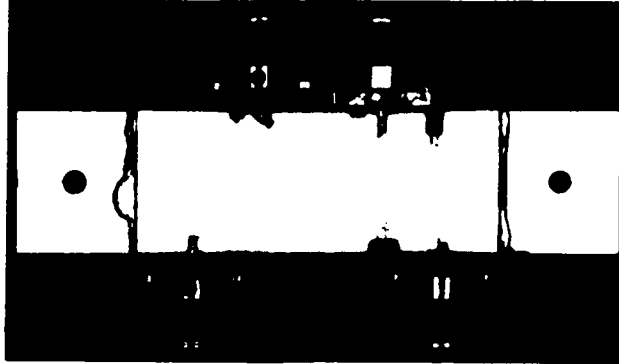


Fig. 2 Photograph of the hybrid

signals appearing at port 3, 4, and  $I$  can be obtained as

$$\text{Signal at port 3, } V_3 = -\sin \theta \sin^2 \theta e^{-j3\beta l} \quad (1)$$

$$\text{Signal at port 4, } V_4 = \cos \theta e^{-j3\beta l} \quad (2)$$

$$\text{Signal at port } I, V_I = j \sin \theta \cos 2\theta e^{-j3\beta l} \quad (3)$$

For  $\theta = \pi/4$  at band center, for a 3-dB hybrid, (1)-(3) become

$$V_3 = -0.707 e^{-j3\beta l} \quad (4)$$

$$V_4 = 0.707 e^{-j3\beta l} \quad (5)$$

$$V_I = 0. \quad (6)$$

Thus the signals appearing at ports 3 and 4 have a phase difference of  $180^\circ$  and are equal in magnitude which is  $\sqrt{2}$  below the input signal (3 dB below in power). Port  $I$  is an isolated port since the signal appearing at port  $I$  is zero.

#### Case 2: Input at Sum Port

In this case, the signal is fed at port 2 (Fig. 1) and port 1 is theoretically isolated. The signals appearing at ports 3, 4, and  $I$  can be obtained as

$$\text{Signal at port 3, } V_3 = j \cos \theta \sin 2\theta e^{-j3\beta l} \quad (7)$$

$$\text{Signal at port 4, } V_4 = j \sin \theta e^{-j3\beta l} \quad (8)$$

$$\text{Signal at port } I, V_I = \cos \theta \cos 2\theta e^{-j3\beta l} \quad (9)$$

For  $\theta = \pi/4$  at band center, for a 3-dB hybrid, (7)-(9) become

$$V_3 = j 0.707 e^{-j3\beta l} \quad (10)$$

$$V_4 = j 0.707 e^{-j3\beta l} \quad (11)$$

$$V_I = 0. \quad (12)$$

Thus signals appearing at ports 3 and 4 are in phase having equal amplitude each 3 dB below the input power. Port  $I$  is an isolated port and is match terminated.

In both cases, the phase difference between two output ports is independent of frequency. However, the amplitude is frequency dependent, since the coupling angle  $\theta$  is frequency dependent. The bandwidth of the hybrid will be slightly less than the bandwidth of each  $90^\circ$  hybrid used. A  $90^\circ$  interdigitated hybrid has over an octave bandwidth.

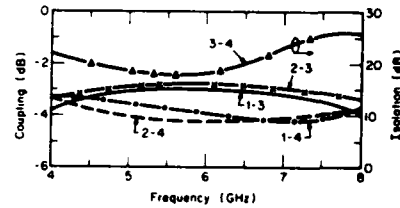
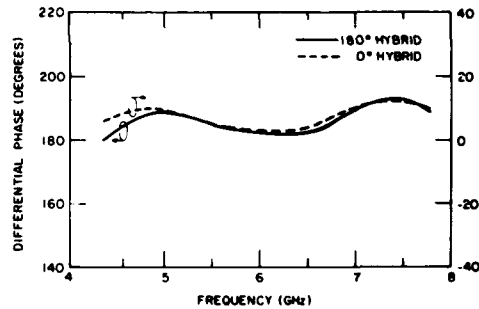


Fig. 3 Variation of coupling and isolation between different ports with frequency of the hybrid

Fig. 4 Variation of differential phase with frequency for two cases of  $180^\circ$  and  $0^\circ$  hybrids.

### III. EXPERIMENTAL RESULTS

The hybrid shown in Fig. 1 consists of three 3-dB  $90^\circ$  hybrids. The design of an interdigitated,  $90^\circ$  hybrid is done using the well-documented theory [6], [7]. We have fabricated this hybrid on a 25-mil-thick alumina substrate. The photograph of the hybrid is shown in Fig. 2. Fig. 3 shows the coupling between different ports of the hybrid. The isolation between two output ports is better than 18 dB. The powers of the two output ports differ by less than 1.5 dB and the insertion loss of the hybrid is less than 0.5 dB over the 4-8-GHz band. The variation of the phase with frequency is presented in Fig. 4, for both cases, when the signal is fed at the different ports or sum port, resulting in two output signals which are  $180^\circ$  out of phase or in phase, respectively. The maximum VSWR at the different ports is 1.4 over the band.

## IV. CONCLUSIONS

We have presented an analysis and experimental results of a  $180^\circ$  hybrid. This hybrid has been realized on alumina substrate. It has a bandwidth of 3 GHz over the 4-8-GHz band with a loss of 0.5 dB, an isolation of  $>18$  dB, and a phase unbalance of  $\pm 7^\circ$ . The hybrid reported here is compatible to monolithic integration on GaAs substrates.

## REFERENCES

- [1] H. Seidel, "Hybrid coupled amplifier," U. S. Patent 3 423 688, Jan. 21, 1969.
- [2] H. J. Hindin and A. Rosenzweig, "3-dB couplers constructed from two tandem connected 8.34 dB asymmetric couplers," *IEEE Trans. Microwave Theory Tech.*, vol. MTT-16, no. 2, pp. 125-126, Feb. 1968.
- [3] J. P. Shelton, J. Wolfe, and R. C. Van Wagoner, "Tandem couplers and phase shifters for multi-octave bandwidths," *Microwaves*, vol. 4, pp. 14-19, Apr. 1965.
- [4] G. Lennart Nyström, "Synthesis of broadband 3-dB hybrids based on the two-way power divider," *IEEE Trans. Microwave Theory Tech.*, vol. MTT-29, no. 3, pp. 189-194, Mar. 1981.
- [5] W. S. Metcalf, "Cascading 4-port networks," *Microwave J.*, vol. 12, pp. 77-82, Sept. 1969.
- [6] P. O. Wer, "Design equations for an interdigitated directional coupler," *IEEE Trans. Microwave Theory Tech.*, vol. MTT-23, pp. 253-255, Feb. 1975.
- [7] A. Presser, "Interdigitated microstrip coupler design," *IEEE Trans. Microwave Theory Tech.*, vol. MTT-26, no. 10, pp. 801-806, Oct. 1978.

DISTRIBUTION LIST  
Contract N00014-79-C-0568

Code 414	4	Dr. Mike Driver	1
Office of Naval Research		Westinghouse Research and	
Arlington, VA 22217		Development Center	
Naval Research Laboratory		Beulah Road	
1555 Overlook Ave., S.W.		Pittsburgh, PA 15235	
Washington, D.C. 20375		Dr. D. Richard Decker	1
Code 6811	1	Rockwell International	
6850	1	Science Center	
6820	1	P.O. Box 1085	
Defense Documentation Center	12	Thousand Oaks, CA 91360	
Building 5, Cameron Station		Dr. C. Krumm	1
Alexandria, VA 22314		Hughes Research Laboratory	
Dr. Y. S. Park	1	3011 Malibu Canyon Road	
AFWAL/DHR		Malibu, CA 90265	
Building 450		Mr. Lothar Wandinger	1
Wright-Patterson AFB		ECOM/AMSEL/TL/IJ	
Ohio 45433		Fort Monmouth, NJ 07703	
ERADCOM	1	Dr. Harry Wieder	1
DELET-M		Naval Ocean Systems Center	
Fort Monmouth, NJ 07703		Code 922	
Texas Instruments	1	271 Catalina Blvd.	
Central Research Lab		San Diego, CA 92152	
M.S. 134		Dr. William Lindley	1
13500 North Central Expressway		MIT	
Dallas, TX 75265		Lincoln Laboratory	
Attn: Dr. W. Wisseman		F124 A, P.O. Box 73	
Dr. R. M. Malbon/M.S. 1C	1	Lexington, MA 02173	
Avantek, Inc.		Commander	1
3175 Bowers Ave.		U.S. Army Electronics Command	
Santa Clara, CA 94303		V. Gelnovatch	
Mr. R. Bierig	1	(DRSEL-TL-IC)	
Raytheon Co.		Fort Monmouth, NJ 07703	
28 Seyon Street		RCA	1
Waltham, MA 02154		Microwave Technology Center	
Dr. R. Bell, K-101	1	Dr. F. Sterzer	
Varian Associates, Inc.		Princeton, NJ 08540	
611 Hansen Way			
Palo Alto, CA 94304			

Hewlett-Packard Corp. Dr. Robert Archer 1501 Page Road Palo Alto, CA 94306	1	Dr. Ken Weller MS/1414 TRW Systems One Space Park Redondo Beach, CA 90278	1
Watkins-Johnson Co. E. J. Crescenzi, Jr./ K. Niclas 3333 Hillview Ave. Stanford Industrial Park Palo Alto, CA 94304	1	Professor L. Eastman Phillips Hall Cornell University Ithaca, NY 14853	1
Commandant Marine Corps Scientific Advisor (Code AX) Washington, D.C. 20380	1	Professors Hauser and Littlejohn Dept. of Electrical Engr. North Carolina State University Raleigh, NC 27607	1
Communications Transistor Corp. Dr. W. Weisenberger 301 Industrial Way San Carlos, CA 94070	1	Professor J. Beyer Dept. of Electrical & Computer Engr. University of Wisconsin Madison, WI 53706	1
Microwave Associates Northwest Industrial Park Drs. F. A. Brand/J. Saloom Burlington, MA 01803	1	Professors Rosenbaum & Wolfe Semiconductor Research Lab Washington University St. Louis, MO 63130	1
Commander, AFAL AFWAL/AADM Dr. Don Rees Wright-Patterson AFB, OH 45433	1	W. H. Perkins Electronics Lab 3-115/B4 General Electric Co. P.O. Box 4840 Syracuse, NY 13221	1
Professor Walter Ku Phillips Hall Cornell University Ithaca, NY 14853	1	Bryan Hill AFWAL/AADE Wright-Patterson AFB, OH 45433	1
Commander Harry Diamond Laboratories Mr. Horst W. A. Gerlach 800 Powder Mill Road Adelphia, MD 20783	1	H. Willing/Radar Directorate BMD - Advanced Tech. Center P.O. Box 1500 Huntsville, AL 35807	1
Advisory Group on Electron Devices 201 Varick Street, 9th Floor New York, NY 10014	1		

**FILMED**  
**8**